PREDICTION OF REACTION LINES IN A PROTOPLANETARY DISK: 3D MONTE CARLO SIMULATION.

L. Ishizaki[1*], S. Tachibana[1], S. Ida[2], T. Okamoto[2] and D. Yamamoto[3], [1] Department of Earth and Planetary Science, The University of Tokyo, Hongo, Tokyo 113-0033, Japan, *E-mail: r.ishizaki@eps.s.u-tokyo.ac.jp, [2] Earth-Life Science Institute, Tokyo Institute of Technology, Meguro, Tokyo 152-8550, Japan, [3]Department of Earth and Planetary Sciences, Faculty of Sciences, Kyushu University, Nishi-ku, Fukuoka 819-0395, Japan.

Introduction: Dust particles in protoplanetary disks experience various physicochemical conditions through their accretional and diffusive transport. For instance, amorphous silicate dust particles crystallize by heating in the disks. The 3D Monte Carlo simulation of crystallization of amorphous silicate dust in the steady accretion disk [1] showed that crystallization occurs at a certain temperature (annealing line), considering the crystallization kinetics. Okamoto and Ida [2] showed that crystallization at the annealing line and the diffusive transport of crystallized dust result in the radial distribution of crystalline silicate dust in the disks. Similar discussion was made through the 3D Monte Carlo simulation for accumulation of radicals in amorphous ice by UV photon irradiation at the upper part of disks [3].

A variety of irreversible/reversible chemical reactions that dust experiences form the radial gradient of chemical properties of dust in the disks [e.g., 1–3]. However, no systematic and comprehensive investigation has been made for various chemical reactions occurring at different temperatures and rates in protoplanetary disks. In this study, we focus on prediction of reaction lines for irreversible reactions of dust with different reaction parameters in steady accretion disks.

Methods: The steady accretion disk model, heated by uniform viscous heating (α-viscosity model [4]) is adopted [3]. We also consider the vertical structure of disk temperature with viscous heating proportional to the disk gas density. The dust opacity is assumed to be 2.5 cm^2 g^{-1} and the central star is assumed to have a solar mass $M_\odot$. We adopted α of 10^{-2} and 10^{-3} and the steady accretion rate $\dot{M}$ of 10^{-6}, 10^{7} and 10^{-8} $M_\odot$ yr^{-1}.

Monte Carlo Simulation. We performed three-dimensional Monte Carlo simulations to evaluate trajectories of dust particles that move around by advection and diffusion, well coupled with disk gas [1, 2, 5]. Ten thousand dust particles were released at the disk midplane near H_2O snowline for each parameter set. The calculations continued for 10^6 years.

Reactions. We examined progresses of fictitious irreversible reactions that are given by the Johnson-Mehl-Avrami (JMA) equation [6, 7]:

$$X = 1 - \exp\left[-\left(\frac{t}{\tau}\right)^{n}\right], \tag{1}$$

where X is the progress degree of each reaction, t is the elapsed time, and n is the Avrami index.

The characteristic reaction timescale, τ, is given by

$$\tau = \left[\nu_0 \exp\left(-\frac{E_\mathrm{a}}{RT}\right)\right]^{-1}, \tag{2}$$

where $\nu_0$is the pre-exponential factor, E_a is the activation energy, and R is the gas constant. The degree of reaction, X, is set to be zero at the release from the snowline. After that, for each timestep of the Monte Carlo simulation, the increment δX calculated by the differentiated JMA equation with local T at the instantaneous position of the particle is added to X. In order to simulate a wide variety of chemical reactions, 270 runs with the parameters in the ranges of the Avrami index n of 0.5-4.0, the logarithm of pre-exponential factor ln(ν_0 [s^{-1}]) of 10–60, and the activation energy E_a of 50–800 kJ mol^{-1} were performed.

The highest temperature ($T_\mathrm{max}^{X_\mathrm{rec}}$) that each particle experienced before the degree of reaction X exceed a certain level X_rec (0.8, 0.9, or 0.99) was recorded for discussion of reaction lines.

Results & Discussion: Figure 1 shows a histogram of $T_\mathrm{max}^{X_\mathrm{rec}}$, whose bin width was determined by Scott's choice [8] for each set of disk and reaction parameters. The distributions of $T_\mathrm{max}^{X_\mathrm{rec}}$ were fitted to the log-normal distribution to obtain the mode temperatures and the dispersions, which are found to be nearly equal to the shape parameter (σ) of the log-normal distribution (the standard deviation of the logarithm of the distribution). We here use the mode temperature of $T_\mathrm{max}^{X_\mathrm{rec}}$ distribution as the reaction line temperature (T_line) and the dispersion ($\Delta T/T_\mathrm{line}$) as the width of reaction lines.

The T_line and its dispersion depend on both reaction parameters and disk parameters. The T_line increases as E_a increases or ν_0 decreases because a reaction occurs more effectively with a larger E_a or a smaller ν_0 at higher temperatures (Eq. 2). The dispersion of T_line increases as ν_0 decreases but it hardly depends on E_a counterintuitively. The T_line is higher for a larger X_rec and a smaller n for the same E_a and ν_0, although the dependence on X_rec and n is not large compared to other reaction parameters. We also found that the T_line shows weak positive and negative dependences with the disk parameters, α and $\dot{M}$, respectively and $\Delta T/T_\mathrm{line}$ does not depend on the disk parameters.

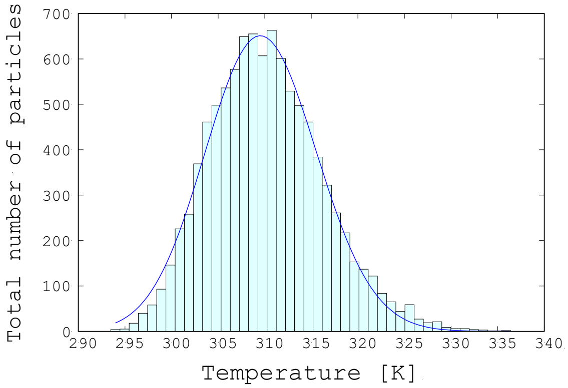

Figure 1. A histogram of the highest temperatures ($T_{\rm max}^{X_{\rm rec}}$) that each particle experiences until when $X_{\rm rec}$ exceeds 0.8 for a reaction with ln(ν_0[s^{-1}])=20, $E_{\rm a}$=100 kJ/mol, and n=1.0. The disk parameters are $\alpha=10^{-2}$ and $\dot{M}=10^{-7}\,M_\odot$ yr^{-1}. In this case, $T_{\rm line}$ of 310 K and $\Delta T/T_{\rm line}$ of 0.0193 are obtained.

We have derived semi-analytical formulas for the reaction line temperature and its dispersion that successfully reproduce the numerical results, by comparing between a reaction timescale and a local diffusive transport timescale of dust particles. Dust particles complete the reaction if they stay in the region at a certain range of temperature, which is high enough for effective reaction, before they leave the region by diffusion.

The formula for "a reaction line" is given as a function of the reaction parameters, n, ν_0, $E_{\rm a}$, $X_{\rm rec}$, and the disk parameters, α and $\dot{M}$. First, the rough estimate of the reaction-line temperature, which is determined only by the reaction parameters, is given by

$$T_{\rm line,0}=\frac{E_{\rm a}}{R}[16.15-\ln C_X+\ln(\nu_0\ [s^{-1}])]^{-1}\ {\rm K}\quad(3)$$

where $C_X=(1/n)[-\ln(1-X_{\rm rec})]^{-(n-1)/n}$ for $n<1$, and $C_X=1/n$ for $n\geq 1$. The width of reaction-line temperature, $\sigma\simeq\Delta T/T_{\rm line}$, is given by

$$\sigma=0.72\times[16.15-\ln C_X+\ln(\nu_0\ [s^{-1}])]^{-1}.\quad(4)$$

Using Eqs. 3 and 4, the more detailed final formula including fine adjustment due to the disk parameters is given by

$$\begin{aligned}T_{\rm line}=\frac{E_{\rm a}}{R}\Bigg[&16.15-\ln C_X+\ln(\nu_0\ [s^{-1}])\\&-\frac{14}{9}\ln\left(\frac{T_{\rm line,0}}{10^3\ {\rm K}}\right)+2\ln\left(\frac{\sigma}{0.0162}\right)\\&-\frac{10}{9}\ln\left(\frac{\alpha}{10^{-2}}\right)+\frac{2}{9}\ln\left(\frac{\dot{M}}{10^{-7}M_\odot\ {\rm yr}^{-1}}\right)\Bigg]^{-1}\ {\rm K}.\quad(5)\end{aligned}$$

These formulas reproduce the numerical results within 5.5% for $T_{\rm line}$ and 24% for σ in the whole reaction and disk parameter ranges that we tested.

Figure 2 shows the numerical results of the $T_{\rm max}$ distributions (red solid lines) and the predicted ones, the log-normal distributions with $T_{\rm line}$ (Eq. 5) and σ (Eq. 4). This demonstrates that our formulas for irreversible chemical reaction gives a good estimate of $T_{\rm line}$ in a steady accretion disk in a wide range of temperature as long as the rate is expressed with the JMA equation. The $T_{\rm line}$ for various reactions can be a powerful tool to understand distributions of materials that experience different chemical processes in protoplanetary disks.

References: [1] Ciesla F. J. (2011) *ApJ, 740,* 9-41. [2] Okamoto T. and Ida S. (2022) *ApJ, 928,* 171-183. [3] Ciesla F. J. and Sandfors. S. A. (2012) *Science,* 336, 452-454. [4] Shakura, N. I. and Sunyaev, R. A. (1973) *A&A, 24,* 337–355. [5] Ciesla F. J. (2010) *ApJ, 723,* 514-529. [6] Avrami M. (1939) *J. Chem. Phys., 7,* 1103-1112. [7] Johnson W. A. and Mehl R. F. (1939) *Trans. AIME, 135,* 416-442. [8] Scott D. W. (1979) *Biometrika, 66, 3,* 605-610.

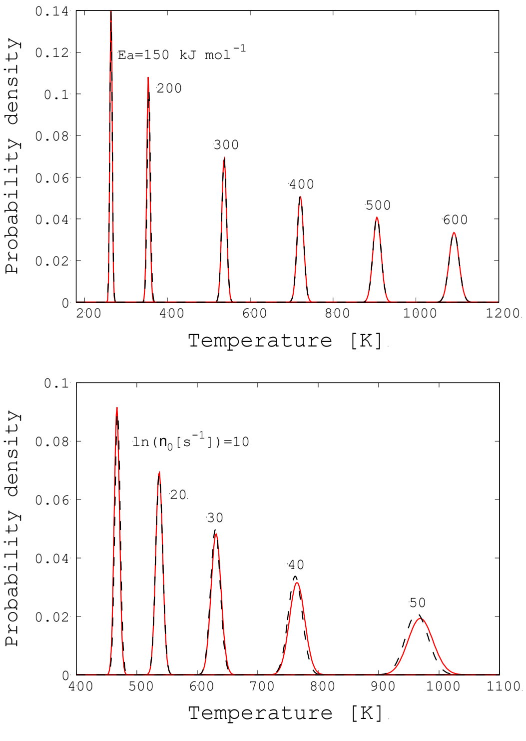

Figure 2. The histograms of $T_{\rm max}^{X_{\rm rec}}$ ($X_{\rm rec}$=0.99) for various chemical reactions (red solid curves) compared with the predicted distributions (black dashed curves). Reactions with various activation energies (ln(ν_0[s^{-1}])=50, n=1.5) (upper panel). Reactions with various pre-exponential factors ($E_{\rm a}$=300 kJ mol^{-1}, n = 1.5) (lower panel). The disk parameters are $\alpha=10^{-2}$ and $\dot{M}=10^{-6}\,M_\odot$ yr^{-1}.